The autopsy revealed hypoplasia of the bone marrow and lingual lesions characterized by epithelial proliferation associated with papillary atrophy and nerve degeneration (*8*). The liver was normal.

On the basis of the foregoing observations, folic acid was administered to niacin-, riboflavin-, pyridoxine-, and pantothenic acid-deficient dogs. Given alone, it failed to bring about any observable effect; nor did it enhance the response to the administration of niacin, riboflavin, pyridoxine, and pantothenic acid in the deficient dogs. Similarly, it did not have any effect when it was given to the control animals.

It appears that some dogs may require folic acid preformed in the diet. The deficiency syndrome is characterized by hypoplasia of the bone marrow, hypochromic anemia with a tendency to microcytosis, and glossitis.

References and Notes

1. *Nutritional anemia*, A. Lejwa, Ed. (Robert Gould Research Fdn., 1947).
2. W. A. Krehl and C. A. Elvehjem, *J. Biol. Chem.* **158**, 173 (1945).
3. W. A. Krehl *et al.*, *Arch. Biochem.* **11**, 363 (1946).
4. W. R. Ruegamer *et al.*, *J. Nutrition* **36**, 425 (1948).

5. This study was supported by a grant from the National Institutes of Health, U.S. Public Health Service.

6. Cobione, Merck and Co.
7. Fovelite, Lederle Laboratory.

8. D. Afonsky, *Oral Surg., Oral Med., Oral Pathol.*, in press.

29 June 1954.

Application of Mercury-Intrusion Method for Determination of Pore-Size Distribution to Membrane Filters

Edith Honold and Evald L. Skau

Southern Regional Research Laboratory, New Orleans, Louisiana

The mercury-intrusion method for determining pore-size distribution is a dilatometric method (*1*) based on the employment of external pressure to overcome the forces of surface tension which prevent the entrance of the nonwetting liquid mercury into the pores of an immersed sample (*2*). The equation

$$pr = -2\sigma \cos \theta \qquad (1)$$

relates the applied pressure p to the radius r of a circular aperture through the coefficient of surface tension σ of mercury and its contact angle θ with respect to the material under test. Recent reports from this laboratory (*3*) have presented the results of the application of this method to cotton textile materials (*4–6*), assuming values for σ and θ that reduce Eq. 1 to

$$pr = 105.6, \text{lb } \mu/\text{in.}^2, \qquad (2)$$

where p is the absolute pressure (lb/in.^{2}) and r is in microns. In this report, these assumptions are examined in the light of the data obtained on hydrosol-type membrane filters whose pore-radius dimensions presumably lie within a limited range.

These filters have been described as highly porous cellulose ester structures containing numerous uniform and submicroscopic channels, whose apertures on the upper surface of the filters are smaller than those on the lower surface, and whose pore size can be controlled in the manufacturing process (*7–11*). The particular variety used for this experiment was Millipore Filters, Type HA (hydrosol assay) (*12*), which have been shown to retain particles as small as 0.3 to 0.5 μ in diameter dispersed in water (*13*). Thus, the limiting radius of the smaller or upper aperture is set at 0.15 to 0.25 μ. From the reported frequency of pores per unit surface (*8, 11*), the limiting radius of the larger and lower aperture can be estimated to be 0.7 μ or less. Both dimensions are based on the assumption that the pores are approximately circular.

The specimens were taken from two different lots representing slightly different ranges with respect to manufacturing control, so that one (sample A) showed a greater resistance to flow than the other (sample B).

The pore-size distribution measurements were made with a porometer (*14*), which permits the estimation of the total void volume within the boundaries of the sample as well as the density of its structural material. The procedure was essentially the same as described previously (*6*) in that a sample (two or more filter leaves)was placed within the porometer chamber, immersed in mercury, and pressure was applied to cover the range from 1.32 to 1015 lb/in.^{2}. Assuming that all the void spaces were filled with mercury at 1015 lb/in.^{2}, the measured bulk volume per leaf at that pressure is equal to the volume of the filter substance (Table 1). From the weight of the leaf, the calculated density of the filter substance was 1.51 g/cm^3 for both samples A and B. The porosity of the original filter leaf—the percentage of void within its boundaries—was estimated from the bulk densities measured at 1.32 and 1015 lb/in.^{2} and had a value of 79 percent in both cases. This value is in agreement with the 75 to 90 percent values reported in the literature (*8, 10, 11, 13*).

The distribution curves for the two samples practically coincide between 80 and 0.7 μ effective radius,

Table 1. Porometer data for millipore filters (average for single leaf).

	Sample A	Sample B
Bulk volume at 1.32 lb/in.^{2} and 80 μ (cm^3)	0.2655	0.2628
Bulk volume at 1015 lb/in.^{2} and 0.1 μ (cm^3)	.0564	.0547
Total void volume, by difference (cm^3)	.2091	.2081
Percentage void volume (porosity)	79	79
Weight of leaf (g)	.0850	.0826
Density of leaf at 1015 lb/in.^{2} (g/cm^3)	1.51	1.51
Pore-radius position of peak of distribution curve (μ)	0.48	0.58

which corresponds to a pressure range of 1.32 to 150 lb/in.^{2}. Approximately 10 percent of the total experimental void volume is filled by the time the pressure reaches 150 lb/in.^{2}, owing in part, most probably, to the compression of the samples as a whole. At higher pressures, the rate of filling of the void volumes increases rapidly, as is shown by the sharp rise to a peak in each distribution curve, and then gradually decreases so that each curve approximates the base line at 0.1 μ or 1015 lb/in.^{2} (Fig. 1). The data place about 90 percent of the total experimental void volume within a radius range of 0.7 to 0.1 μ, thus agreeing with the channel dimensions as predicted in a preceding paragraph from the description of the filters.

In this region, the void volumes per leaf—the areas beneath the curves (*1*)—are approximately equal for the two samples, but the distribution according to pore-radius dimensions is different. Sample A shows a consistently smaller effective radius than sample B, and the peaks of the distribution curves occur at 0.48 and 0.58 μ, respectively. Since the porosities of the samples are equal, 79 percent, the distribution in the radius range below 0.7 μ is in qualitative agreement with the permeability data (*15*), which show that sample A has a resistance to flow 33 percent greater than sample B at various pressure differentials.

If the channels are cylindrical, the porometer data indicate that the radius dimensions of the channels in sample A are smaller than those of sample B. An alternate interpretation could ensue from a consideration of the definition of effective radius: the radius of a hypothetical circular pore which would admit mercury at the same pressure as that required to force passage through the actual pore regardless of its cross-sectional shape (*5*). The channels in sample A may have the same cross-sectional areas as those in sample B, but they may deviate more from a circular toward an elliptical cross section. They therefore would exhibit a smaller effective radius and screen out smaller particles and, likewise, would present more resistance to flow, since flow is influenced similarly by the cross-sectional shape of the channels.

In general, the results indicate that the effective pore sizes, calculated from mercury-intrusion measurements on the basis of Eq. 2 and its underlying assumptions, are reasonably accurate. The pore-size distribution data obtained by this method should prove useful in theoretical and practical investigations dealing with the characteristics of these and of similar type filters, and, in fact, of a variety of porous materials.

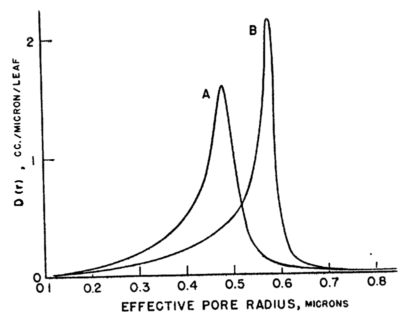

Fig. 1. Pore-size distribution curve, that is, distribution function $D(r)$ versus effective pore radius.

References and Notes

1. H. L. Ritter and L. C. Drake, *Ind. Eng. Chem. Anal. Ed.* **17**, 782 (1945).
2. E. W. Washburn, *Proc. Natl. Acad. Sci.* (*U.S.*) **7**, 115 (1921).
3. One of the laboratories of the Southern Utilization Research Branch, Agricultural Research Service, U.S. Department of Agriculture.
4. E. G. Burleigh, Jr., *et al., Textile Research J.* **19**, 547 (1949).
5. E. Honold and E. L. Skau, *ibid.* **21**, 419 (1951).
6. E. L. Skau, E. Honold, and W. A. Boudreau, *ibid.* **23**, 798 (1953).
7. H. F. Clark *et al., Public Health Repts.* (*U.S.*) **66**, 951 (1951).
8. A. Goetz and N. Tsuneishi, *J. Am. Water Works Assoc.* **43**, 943 (1951).
9. H. F. Clark and P. W. Kabler, *Am. J. Public Health* **42**, 385 (1952).
10. A. Goetz, *ibid.* **42**, 389 (1952).
11. ———, R. H. Gilman, and A. M. Rawn, *J. Am. Water Works Assoc.* **44**, 471 (1952).
12. Obtained from Lovell Chemical Co. Mention of names of firms or trade products does not imply endorsement or recommendation by the U.S. Department of Agriculture over other firms or similar products not mentioned.
13. J. H. Bush, *Sci. Monthly* **75**, 303 (1952).
14. W. R. Purcell, *J. Petroleum Technol.* **1**, No. 2, Tech. Paper No. 2544, 39 (1949); *Am. Inst. Mining Met. Engrs., Petroleum Trans.* **186**, 39 (1949).
15. Data supplied by manufacturing company, private communication.

25 June 1954.

Processes of Motion Perception

Rayford T. Saucer*

Department of Psychology, Georgia Institute of Technology, Atlanta, Georgia

In an earlier paper (*1*) I discussed the nature of lateral transfer of perceptual organizations. It is believed that a matrix theory of perception can be used as the basis of a unified theory of motion perception. Present theories commonly divide motion perception into two parts. Real motion, in which the perception of movement arises from the movement of an object in real space, is considered different from subjective motion, in which the perceptual organization arises out of the given spatiotemporal complex of stationary stimuli.

It is felt that the two can be related or unified by recourse to a theory of a dual set of organizations, the one corresponding to the perception of motion and the other to the perception of pattern or detail. The basis for this theory lies in two sets of phenomena observed in apparent motion studies.

It is well known that apparent motion perception can be optimized for a particular set of dynamic variables. Below the optimal point, motion tends to disappear and is replaced by the successive appearance of the stimuli. Above the optimal point, it is replaced by simultaneous appearance of the stimuli. Under stimulus conditions reported (*1*), the second stage is characterized by a phenomenon that I have called "Omega." The Omega complex is reported as (i) a black shutter or door that opens to reveal the light source, (ii) a hole in nothing, and (iii) as various